Astron. Astrophys. 345, 181–186 (1999)

ASTRONOMY AND ASTROPHYSICS

The ISO spectrum of the young star HD 142527⋆

K. Malfait[1], **C. Waelkens**[1], **J. Bouwman**[2], **A. De Koter**[2], **and L.B.F.M. Waters**[2]

[1] Instituut voor Sterrenkunde, K.U.Leuven, Celestijnenlaan 200B, B-3001 Leuven, Belgium
[2] Astronomical Institute 'Anton Pannekoek', University of Amsterdam, Kruislaan 403, 1098 SJ Amsterdam, The Netherlands

Received 21 October 1998 / Accepted 16 February 1999

Abstract. We present a detailed analysis of SWS (2.35–45 μm) and LWS (43–200 μm) spectra obtained with the Infrared Space Observatory (ISO) (Kessler et al. 1996) of the dusty circumstellar disk surrounding the isolated young Fe star HD 142527. Two dust populations can be clearly discriminated: a warm component which is dominated by very strong silicate emission at 10 μm, but in which C-rich dust is observable as well, and a cool component, of which the spectrum is dominated by O-rich dust features (C-rich dust not cause obvious features in the far infrared). Besides silicates, crystalline water-ice and hydrous silicates - which are also found in interplanetary dust particles - are present in the cold circumstellar environment. The ISO spectrum of HD 142527 differs markedly from that of HD 100546 (Malfait et al. 1998b) and other objects in a similar evolutionary stage and with a similar broad-band energy distribution. No clear correlations between the spectral dust signatures and the stellar parameters can be found at the present stage.

Key words: stars: circumstellar matter – stars: individual: HD 142527 – infrared: ISM: lines and bands – inteplanetary medium

1. Introduction

Circumstellar disks surrounding young stars are remnants of the star formation process. The collapse of a molecular cloud leads to the formation of disks with accretion onto a central stellar-like object. These circumstellar disks are thought to disappear on a timescale of several million years (Backman & Paresce 1993). Nevertheless, faint disks surround several main-sequence stars, such as Vega and β Pictoris (Aumann et al. 1984; Gillett 1986), suggesting the presence of a reservoir of bodies, the collisions of which replenish the disk. It is generally assumed that planets may form in these dusty disks (e.g. Beckwith & Sargent 1996). Therefore, it is interesting to study the evolution of these circumstellar dusty disks, which can be observed in the infrared, due to the thermal radiation of the circumstellar dust.

HD 142527 (F7IIIe) is a so-called 'isolated' Herbig Ae/Be star (or Fe star in this particular case): its strong infrared excess and Hα emission argue for a young age, but it is not located in a well known star-forming region. From the Digitized Sky Survey (consulted at http://skys. gsfc.nasa.gov/cgi-bin/skyview_advanced.pl), it can be seen that HD 142527 has a small weak nebulous environment, in which no other but this IRAS-object is present. Thus, it might be a transition object between the youngest, embedded stars and main-sequence objects such as Beta Pic. However, this picture is not confirmed by Hipparcos parallax-measurements of this star, which, confronted to stellar-evolution models, suggest an age $\sim 10^5$ yr (van den Ancker et al. 1998), which is less than the age of several embedded objects.

HD 142527 is an ideal target for infrared spectroscopy, since its circumstellar dust is bright, and since its isolated nature avoids confusion with the loose surroundings that occur for more embedded sources.

2. Observations

Full scans of the spectrum of HD 142527 in the 2.4–45 μm range with the Short Wavelength Spectrometer (SWS) (de Graauw et al. 1996) and in the 43–200 μm range with the Long Wavelength Spectrometer (LWS) (Clegg et al. 1996) on board of ISO have been obtained on March, 1^{st} 1996. The integration times were respectively 2046 and 2441 seconds.

The SWS-spectrum and LWS-spectrum were reduced using the latest version of the standard pipeline. This resulted in a oversampled spectrum in which every single detector (48 for SWS, 10 for LWS) is wavelength- and flux-calibrated. Remaining instrumental effects, such as fringes (periodic flux oscillations) and glitches (cosmic impacts exciting the detector), still had to be corrected for, which has been done using the instrumental analysis packages (IA) provided by the instrument teams. In order to increase the S/N, the most outlying data points have been removed using a statistical rejection criterium with σ=2.5. After aligning the different detector signals and rebinning to the expected resolution (R $\sim$ 300), we obtained the final result. The full SWS-LWS spectrum of HD 142527 is shown in

Send offprint requests to: Koen Malfait, Leuven (koenm@ster.kuleuven.ac.be)

⋆ Based on observations with ISO, an ESA project with instruments funded by ESA Member States (especially the PI countries: France, Germany, the Netherlands and the United Kingdom) and with the participation of ISAS and NASA

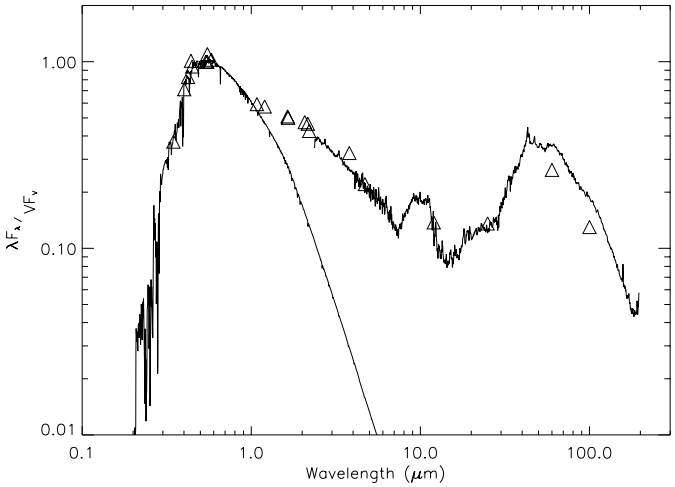

Fig. 1. Spectral energy distribution of HD 142527, normalized to the V-band. UV-continuum fluxes, derived from spectra obtained with the International Ultraviolet Explorer IUE, optical Geneva photometry, near-IR ESO-photometry, near-IR fluxes derived from IRSPEC near-IR spectroscopy obtained at ESO, as well as IRAS broad-band photometry are represented by triangles. A Kurucz-model (T_{eff} = 6250 K, log g = 4.0 and solar metallicity) and the ISO-spectra are overplotted.

HD 142527's spectral energy distribution on Fig. 1. The independently reduced SWS and LWS spectrum match almost perfectly, confirming the detector alignment performed. However, a discrepancy between the LWS-spectrum and the 60 and 100 μm IRAS-fluxes is observed. No explanation for this mismatch has been found.

3. Identification and description

From an earlier photometric study (Malfait et al. 1998a), it is known that the infrared spectrum of HD 142527 is characterized by a warm and a cold component, intersecting at ~ 20 μm. On top of that warm continuum ($\lambda \leq 20$ μm) a silicate bump is clearly visible. Evidence for the 3.3 μm and 6.2 μm UIR bands, usually attributed to PAHs is present as well, though the previously mentioned 3.5 μm band (Waelkens et al. 1996) cannot be confirmed using the latest calibration files (Van Kerckhoven, in prep.). The scientific relevance of the features seen longwards of the silicate emission (between 11 and 16 μm), is questionable. A detailed study of similar features shortward of the 6.2 μm PAH, showed that not all 12 detectors observed the features in both up and down scans, thus one can conclude that these features are spurious. For the features between 11 and 16 μm, a more detailed study should be done to discriminate whether they are real, since also severe memory effects take place in the relevant detectors. This will be done when the PAHs will be discussed in more detail (Van Kerckhoven, in prep.).

In the longer wavelength part of the spectrum, sharp solid state peaks at 43, 47, 50 and the 158 μm-line attributed to forbidden [CII] are visible on top of the very strong continuum flux. A broad feature at 55–75 μm is visible as well.

The sharp peak at 43 μm in combination with the broad band centered at 63 μm, is a characteristic for crystalline H_2O-ice, which seems to be quite common in the environment of young stars and post-AGB stars (Waters et al. 1996; Barlow 1998; Malfait et al. 1998b). If we compare the features of HD 100546 (Malfait et al. 1998b) with those of HD 142527, the $\frac{63\,\mu m}{43\,\mu m}$ strength ratio is drastically higher for the latter. The dust temperature found from continuum modelling is higher for HD 100546 ($T \sim$ 40–210 K) than for HD 142527 ($T \sim$ 30–90 K). This shifts the far infrared dust emission to shorter wavelengths, attenuating the 43 μm peak relatively to the 63 μm peak, and explaining the different band strength ratio.

Table 1. Reference list of optical properties used.

Dust type	Reference
Amorphous silicates	Draine & Lee 1984 Jäger et al. 1994 Dorschner et al. 1995
Crystalline silicates	Mukai & Koike 1990 Koike et al. 1993 Jäger et al. 1998
Hydrous silicates	Koike et al. 1982 Koike & Hiroshi 1990
Metal oxides	Henning et al. 1995
H_2O-ice	Bertie et al. 1969 Warren 1984
Graphite	Laor & Draine 1993

4. Radiative transfer modelling

It is clear from the diversity of spectral features in the near- and far-IR that the dust consists of two spatially divided components. To model this geometry, we have used the dust radiative transfer program `MODUST` (Bouwman & Waters 1998; de Koter et al. in preparation). Currently, `MODUST` solves the radiative transfer equations subject to radiative equilibrium in spherical geometry. A 2D version is presently being developed. The density distribution of one or multiple (physically separated) shells may be freely specified. To take into account the effect of grain size on the extinction properties of the dust a powerlaw grain-size distribution is assumed. In the presented calculations, grains are assumed to be spherical, compact and to consist of a single grain material. A nice feature of the program is a library of optical constants – derived in laboratory measurements – containing about fifty dust species that may contribute to the predicted spectrum. This allows for detailed modelling of ISO spectra. As optical depths in the shells are well below unity, we run the program in the optical thin limit.

This spherical geometry is not correct for our scientific purpose, though because of the optically thin fingerprints of the dust, except for geometrical parameters, the overall results should be consistent.

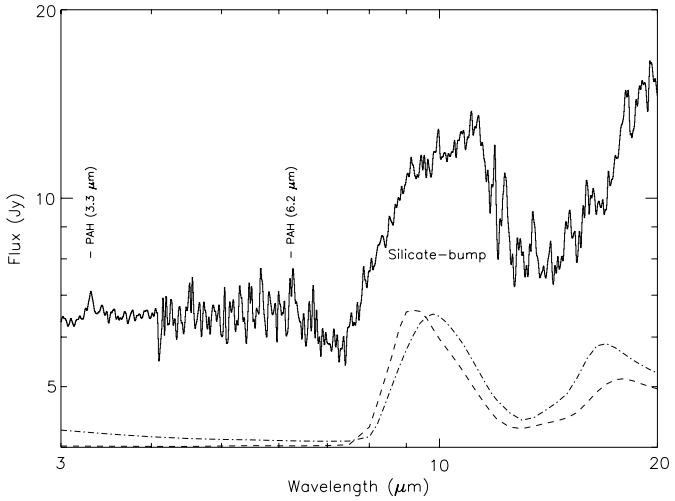

Fig. 2. Short wavelength part of the SWS spectrum of HD 142527. The silicate bump dominates this wavelength range, but also the 3.3 and 6.2 μm PAH bands can be identified. Overplotted are the absorption efficiencies (arbitrary units) for an amorphous pyroxene ($Mg_{0.5}Fe_{0.5}SiO_3$, dashed line) and an amorphous olivine ($Mg_{0.8}Fe_{1.2}SiO_4$, dot-dashed line) (Dorschner et al. 1995). The different noise levels ($\lambda \leq 4$ μm vs. ≥ 4 μm) are caused by the use of different detector materials (de Graauw et al. 1996).

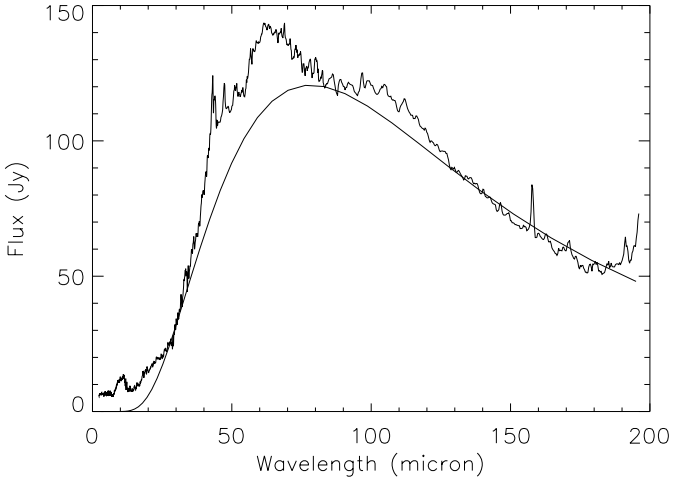

Fig. 3. Far-IR continuum fit of HD 142527, using an optically thin dust model with $Q_\lambda \propto \lambda^{-1}$, $n(r) \propto r^{-1.25\pm0.05}$, an inner and outer disk temperatures of 90 K and 30 K, respectively.

4.1. The hot dust

The first of the two distinct dust populations is located close to the object, and has a dust temperature ranging from 500 to 1500 K.

The dust is mainly composed of silicates. The presence of both olivines (island silicates consisting of SiO_4 tetrahedra linked to each other by divalent cations) and pyroxenes (chain silicates, of which each SiO_4 tetrahedron shares two of its oxygen atoms with its neighbours, resulting in the symbolic formula $Mg_xFe_{1-x}SiO_3$, see Henning 1998) is evident from the broadness of the 10 μm band, from which the shortest (8–10 μm) and longer (9-11 μm) wavelength part can be attributed to respectively pyroxenes and olivines (see Fig. 2). In addition to the amorphous silicate component, crystalline olivine and pyroxene dust has been used in the fit as well. Mg-rich crystalline olivines cause the 11.2 μm emission and can explain the rather noisy shape of the spectrum at 16 μm as well.

FeO has, next to a feature at 20 μm which can partially explain the shape and flux of the spectrum, a strongly rising emissivity at short wavelengths (2–6 μm) and can account for most of the near-IR continuum flux. A graphite component with a small abundance completes the inner part.

4.2. The cold dust

In order to model the second dust population, which is located further out, a first attempt to derive the cold dust temperature has been made using an optically thin dust disk model (Waters et al. 1988; Malfait et al. 1998a). Using an emissivity law $Q_\lambda \propto \lambda^{-1}$, a best fit was found for a dust surface density law dropping as $r^{-1.25\pm0.05}$ and for inner and outer disk temperatures of 90 ± 3 and 30 ± 1 K, respectively (see Fig. 3). In the residuals, we can distinguish a broad feature at 100 μm, in addition to the features mentioned above. The 100 μm band might be present as well in the spectrum of HD 100546, but is much less prominent than in HD 142527 (Waters & Waelkens, 1998). Barlow (1998) also found a band at $\lambda \sim 95$ μm in the spectrum of several evolved objects, such as the planetary nebula NGC 6302, which also shows prominent crystalline H_2O-bands. It is then probable that the 100 μm band is related to H_2O. However, laboratory experiments (Bertie et al. 1969; Moore & Hudson 1994) clearly show that H_2O-ice is not the carrier of the 100 μm band. It is even likely that the bands seen in the diverse spectra are not caused by one single kind of dust, but rather by a family of dust species, resulting in spectral fingerprints at somewhat different wavelengths (NGC 6302 $\leftrightarrow$ HD 142527).

A literature search for optical constants of H_2O-related dust components resulted in identifying a possible carrier for the far-IR feature at 100 μm. Koike el al. (1982) and Koike & Hiroshi (1990) studied hydrous silicates and found that the far-IR spectrum of montmorillonite measured at room temperature is characterized by sharp peaks, the longest wavelength one of them located at 49 μm, and a broad band centered at about 100 μm. The chemical composition of montmorillonite (Koike et al. 1982) is:

$$\left(\frac{1}{2}\mathrm{Ca,Na}\right)_{0.7}\ (\mathrm{Al,Mg,Fe})_4\ (\mathrm{Si,Al})_8\ \mathrm{O}_{20}\ (\mathrm{OH})_4 \cdot \mathrm{n\,H_2O}$$

It has a very definite structure consisting of silicate tetrahedra (arranged in parallel planes and connected at their mutual corners) separated by layers of cations such as Na^+, K^+, Ca^{2+} etc., and layers of what is known as interstitial water. In addition, some of the non-bridging oxygens can be OH^- rather than O^{2-}.

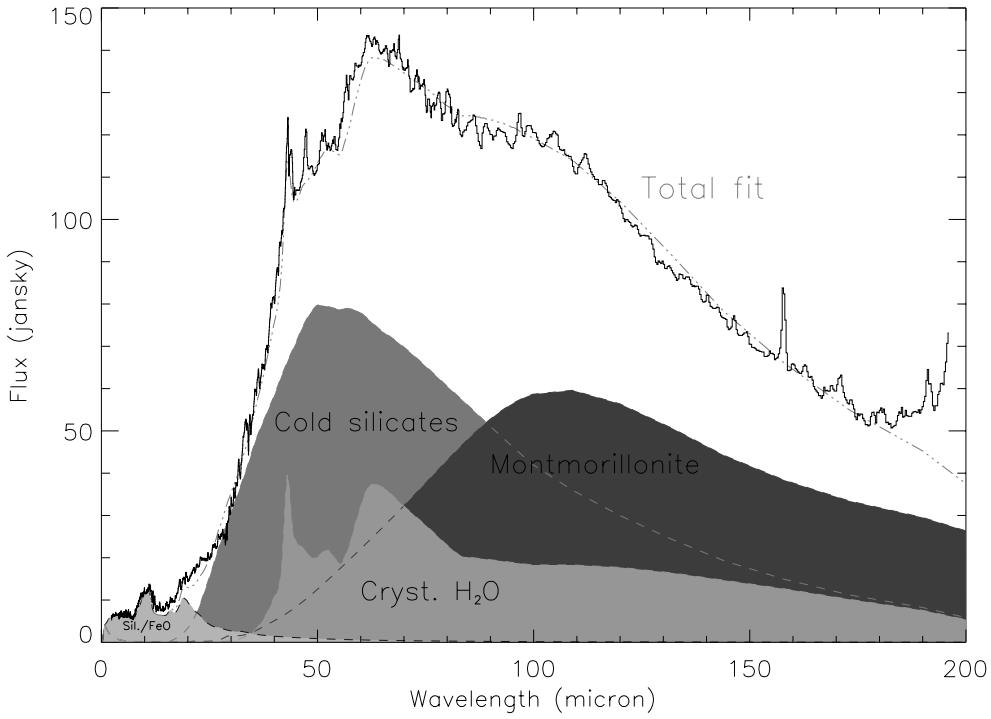

Fig. 4. Modelfit (using MODUST), for details: see text.

We were able to fit the far-IR excess with a mixture composed of 60 % H_2O-ice (of which 90 % is crystalline), 25 % cold amorphous silicates and 15 % montmorillonite.

We independently inserted the three dust components in the model, changing the inner and outer radii of their population, assuming each population to behave independently of the others. The best fit was obtained when the dust temperatures of the three mineral populations agreed very well. This confirms that the dust is mixed and in thermal equilibrium. The dust temperatures (30–60 K) estimated from this radiative transfer modelling are in disagreement with the temperature estimated from black-body modelling (30–90 K), the optical properties of realistic particles being drastically different from $Q_\lambda \propto \lambda^{-1}$.

The dust mass of this cold component is $\sim 5 \cdot 10^{-4}\ M_\odot$, i.e. $\pm\, 10^6$ times more massive than what we estimated from our fit for the warm dust component, using MODUST. If we assume a dust to gas ratio of $\frac{1}{100}$, the circumstellar disk has a mass of the order of a few percent of a solar mass.

4.3. Shortcomings of the modelfit

In Fig. 4, we show the fit we have obtained. Although it matches rather well, we still see some significant discrepancies. The model fails to reproduce the flux level at wavelengths between 12 and 30 μm. Adding a minor fraction of FeO (≤ 1 %) to the cold dust component can solve the lack of flux at 20 μm, but does not explain the total mismatch. Some other explanations could solve the problem. First of all, the model uses a dust density law, which, for each component, starts at a given distance r_{min} from the star and ends at an outer radius r_{max}. In between these two radii, a particle density law $n(r) \propto r^{-m}$ is used, while at the two edges, a smoother density gradient should be used. A second effect is related to the shape of the dust particles. In our fit, we only used spherical particles (Mie-theory, see e.g. Bohren & Huffman 1983), though CDE-effects (continuous distribution of ellipsoids) have a major influence on the optical properties of FeO (but only a minor influence on e.g. silicates), resulting in a much broader feature at 20 μm (Henning et al. 1995). Our assumption to use two spatially separated dust populations might be questionable as well. At 10–25 μm, the predicted flux cannot account for the observed flux, which is up to 5 Jy brighter. This can be caused by the presence of an intermediary dust component with a temperature between 120 and 300 K.

In the far-IR, our model does not reproduce the sharp peaks at 47 and 50 μm. When Koike & Hiroshi (1990) measured the absorption efficiency of montmorillonite, they derived optical constants (n, k) by fitting the experimental results with Lorentz oscillators. Since the peak at 49 μm could not be reproduced this way, it has been neglected and therefore, it is not incorporated in the optical constant set we used. In addition to this, from a comparison of the mass extinction coefficients of montmorillonite at room temperature and at 2 K (Koike et al. 1982), it looks like the 49 μm feature breaks up in two peaks, one at slightly shorter and one at slightly longer wavelength. Although the resolution of these published old measurements is poor, it is tempting to conclude that the 47 μm and 50 μm features present in the spectrum of HD 142527 are again due to montmorillonite. Future laboratory measurements should clarify this matter.

The observations longwards of 180 μm should not be trusted, since in our observing mode, this part of the spectrum is observed with a much lower S/N.

5. Discussion and conclusions

In this paper, we have looked into detail at the ISO spectrum of HD 142527. Although it is currently not possible (model constraints, insufficient laboratory data, ...) to derive the exact circumstellar dust properties, we are able to produce a decent fit, resulting in some ideas on how the circumstellar environment of this pre-main sequence star looks like and how it evolves.

We have shown that in the circumstellar dust disk of the young Fe-star HD 142527, at least two distinct dust populations, of which the coldest has a temperature of only 30 to 60 K, can be distinguished. The dust of the warmest component spans a temperature range from 500 to 1500 K. Not only the temperature but also the composition differs. The warm component is mainly composed of silicates, some of which are crystalline. This crystallization has not occured in the cold dust environment.

On the other hand, warm montmorillonite would display very distinct emission features in the near-IR (e.g. at 6 μm), which are not present. The crystalline silicates being warm, and the hydrous silicates being cold, should not come as a surprise, since the dust condensation temperatures are about 1400 and about 300 K respectively (Larimer & Anders 1967). Since other stars (e.g. HD 100546) do exhibit the characteristic crystalline silicate features at longer infrared wavelenghts, corresponding to much colder dust temperatures, other dust processing mechanisms must already have occurred there.

Hydrous silicates, of which montmorillonite is one example, are known to be present in solar system matter. A study of interplanetary dust particles (IDPs) by Sandford & Walker (1985) shows that IDPs can be divided in three major families, the olivines, the pyroxenes and the layer-lattice silicates. Sandford & Walker studied 26 particles, of which 11 were composed of layer-lattice silicates, such as montmorillonite. From the isotopic enrichments, they concluded that the particles were formed or during the cold molecular phase prior to solar system formation, or during the nebular-protostar phase, where they formed in cold dense regions of the nebula, possibly as a result of alteration of high temperature condensates (olivine and pyroxene) when equilibrated with H_2O (Larimer & Anders 1967; Zaikowski & Knacke, 1975). Sandford & Walker (1985) obtained a fit of the spectrum of comet Kohoutek using 50 % of pyroxene IDPs and 50 % layer-lattice IDPs. A nearly perfect fit of the 10 μm spectrum of comet P/Halley could be obtained as well, using a variety of IDPs, including a small amount of layer-lattice silicates (Bregman et al. 1987). By comparing the spectrum of the protostellar object W33 with the layer-lattice IDP Skywalker, Sandford & Walker (1985) demonstrated that hydrous silicates are present outside the solar system as well. Condensation of hydrous silicates in the outflow of supernova SN 1987A has also be postulated (Timmermann & Larson 1993).

In order to study the evolution circumstellar dust undergoes when a star descends towards the main sequence, we compared the dust characteristics of HD 142527 with those of HD 100546 and HD 179218, two isolated Herbig Ae/Be stars with ages of more than 10^7 years and about 10^5 years respectively, which means hundred times older and of approximately the same age of HD 142527, respectively.

The spectrum of HD 100546 (B9V) is characterized by a series of mid infrared emission peaks, which can be attributed to crystalline forsterite (Mg_2SiO_4), with temperatures as low as 210 K. Also a massive 50 K component is present, accounting for the 69 μm forsterite spectral feature that has been observed (Malfait et al. 1998b). Crystalline H_2O-ice is present as well in the environment of this main sequence star. The presence of a small amount of hydrous silicates is likely, some evidence for the 100 μm features is present (Waters & Waelkens, 1998). That the spectrum of HD 142527 is partially characterized by cold hydrous silicates, while the radiation of the cold dust surrounding HD 100546 is dominated by crystalline silicates is likely to be an age effect. This hypothesis is strengthened by the lack of features caused by crystalline silicates in the spectra of more embedded Herbig Ae/Be stars (Waters, van den Ancker, private communication).

HD 179218 (B9e) on the other hand, has an age similar to that of HD 142527. However, its spectrum resembles that of HD 100546 more than it resembles the spectrum of HD 142527 (Waelkens et al. 1998). Although no detailed modelling has been performed yet, the presence of cold crystalline silicates (both olivines and pyroxenes) is obvious. Since no LWS-spectrum of this star has been taken, we cannot confirm or exclude the presence of H_2O-ice (there is a peak present at 43 μm, but this might be caused by pyroxenes as well) and of hydrous silicates. IRAS photometry does not help here. From these three stars, we cannot detect a clear correlation between age and dust composition. The dust processing mechanisms or time scales on which these processes occur seem to differ from star to star.

What mechanisms do cause crystallization of the silicates? This chemical metamorphosis cannot take place at the low temperatures ($T \leq 300$ K) that result from our modelling. Or is a fraction of the silicate dust already crystallized and/or hydrated before the star and disk form? If so, why do deeply embedded Herbig Ae/Be stars not show these characteristics? Is this an abundance effect? If so, how come these abundances change in time, causing a trend from amorphous towards more ordered mineral structure? Is the presence of hydrous silicates a temperature effect, and are they therefore only present in very cold circumstellar disks (like the one surrounding HD 142527)? How comes HD 142527 is already an 'isolated' Haebe star, and why has the envelope already dissappeared on such a short timescale, much shorter than the age of several embedded objects (van den Ancker et al. 1998)? Does the abundance of H_2O-ice play an important role? To answer these questions, more Haebe objects (both embedded and isolated) should be studied in more detail.

We must point out that the study of only the SWS-spectrum of HD 142527 would have resulted in a totally different interpretation since no evidence for hydrous silicates would have been found. Broad band photometry (such as IRAS) in the far-IR is not sufficient to represent the dust disk continuum flux, but can almost exclusively be attributed to solid state features. As a consequence, dust modelling is necessary to derive reliable physical quantities such as the dust temperature. It turns out

that discriminating between all different silicate minerals is difficult, since they are all characterized by a prominent feature at 10 μm, and often emit strongly at various longer wavelengths. This makes modelling very difficult. An overview paper ordering all laboratory research that has been done on cosmic-like dust particles, would be very useful.

The current effort that is being made to converge the knowledge of laboratory science, solar system research, earth geology and stellar astronomy will probably result in the solution of a lot of the questions remaining in this field.

Acknowledgements. KM acknowledges financial support from the Fund of Scientific Research - Flanders.

References

Aumann H.H., Gillett F.C., Beichman C.A., 1984, ApJ 278, L23
Backman D.E., Paresce F., 1993, Planetesimals and Planets. In: Levy E.H., Lunine J.I. (eds.) Protostars and Planets. The University of Arizona Press, p. 1253
Barlow M.J., 1998, Ap&SS 255, 315
Beckwith S.V.W., Sargent A.L., 1996, Nat 383, 139
Bertie J.E., Labbé H.J., Whalley E., 1969, J.Ch.Ph. 50, 4501
Bohren C.F., Huffman D.R., 1983, Absorption and Scattering of Light by Small Particles. Wiley, New York
Bouwman J., Waters L.B.F.M., 1998, Ap&SS 255, 435
Bregman J.D., Campins H., Witteborn F.C., et al., 1987, A&A 187, 616
Clegg P.E., Ade P.A.R., Armand C., et al., 1996, A&A 315, L38
de Graauw Th., Haser L.N., Beintema D.A., et al., 1996, A&A 315, L49
Dorschner J., Begemann B., Henning T., et al., 1995, A&A 300, 503
Draine B.T., Lee H.M., 1984, ApJ 285, 89
Gillett F.C., 1986, In: Light on Dark Matter. Proceedings of the First Infra-Red Astronomical Satellite Conference, D. Reidel Publishing Co., Dordrecht, p. 61
Henning Th., Begemann B., Mutschke H., Dorschner J., 1995, A&AS 112, 143
Henning Th., 1998, To be published in: Waelkens C., Le Bertre T. (eds.) Asymptotic Giant Branch Stars. Proceedings of IAU Symposium 191
Jäger C., Mutschke H., Begemann B., et al., 1994, A&A 292, 641
Jäger C., Molster F.J., Dorschner J., et al., 1998, A&A 339, 904
Kessler M.F., Steinz J.A., Anderegg M.E., et al., 1996, A&A 315, L27
Koike C., Hiroshi S., 1990, MNRAS 246, 332
Koike C., Hasegawa H., Hattori T., 1982, Ap&SS 88, 89
Koike C., Shibai H., Tuchiyama A., 1993, MNRAS 264, 654
Laor A., Draine B.T., 1993, ApJ 402, 441
Larimer J.W., Anders E., 1967, GeCoA 31, 1239
Malfait K., Bogaert E., Waelkens C., 1998a, A&A 331, 211
Malfait K., Waelkens C., Waters L.B.F.M., et al., 1998b, A&A 332, L25
Mukai T., Koike C., 1990, Icarus 87, 180
Moore M., Hudson R.L., 1994, A&AS 103, 45
Sandford S.A., Walker R.M., 1985, ApJ 291, 838
Timmermann R., Larson H.P., 1993, ApJ 415, 820
van den Ancker M.E., de Winter D., Tjin A Djie H.R.E., 1998, A&A 330, 145
Waelkens C., Malfait K., Waters L.B.F.M., 1998, To be published in: The first International Conference on Comet Hale-Bopp. Special issue of Earth, Moon and Planets
Waelkens C., Waters L.B.F.M., de Graauw M.S., et al., 1996, A&A 315, L245
Warren S.G., 1984, ApOpt 23, 1206
Waters L.B.F.M., Waelkens C., 1998, ARA&A 36, 233
Waters L.B.F.M., Coté J., Geballe T.R., 1988, A&A 203, 348
Waters L.B.F.M., Molster F.J., de Jong T., et al., 1996, A&A 315, L361
Zaikowski A., Knacke R.F., 1975, Ap&SS 37, 3